Chemical Science

EDGE ARTICLE

View Article Online
View Journal | View Issue

Cite this: *Chem. Sci.*, 2019, **10**, 7379

All publication charges for this article have been paid for by the Royal Society of Chemistry

Received 3rd May 2019
Accepted 14th June 2019

DOI: 10.1039/c9sc02167a

rsc.li/chemical-science

Bis(catecholato)silanes: assessing, rationalizing and increasing silicon's Lewis superacidity†

Deborah Hartmann, Marcel Schädler and Lutz Greb *

Although bis(catecholato)silanes have been known for several decades, their substantial Lewis acidity is not yet well described in the literature. Herewith, the synthesis and characterization of multiple substituted bis(catecholato)silanes and their triethylphosphine oxide, fluoride and chloride ion adducts are reported. The Lewis acidity of bis(catecholato)silanes is assessed by *effective* (Gutmann–Beckett, catalytic efficiency), *global* (theoretical and relative experimental fluoride (FIA) and chloride (CIA) ion affinities) and *intrinsic* (electrophilicity index) scaling methods. This comprehensive set of experimental and theoretical results reveals their general Lewis acidic nature and provides a consistent Lewis acidity trend for bis(catecholato)silanes for the first time. All experimental findings are supported by high-level DLPNO-CCSD(T) based thermochemical data and the Lewis acidity is rationalized by complementary chemical bonding analysis tools. Against the common belief that inductive electron withdrawal is the most important criterion for strong Lewis acidity, the present work highlights the decisive role of π-back bonding effects in aromatic ring systems to enhance electron deficiency. Thus, bis(perbromocatecholato)silane is identified and synthesized as the new record holder for silicon Lewis superacids.

Introduction

Lewis acids play a prominent role in all domains of chemistry, such as (bio)organic, organometallic, (bio)inorganic, polymer and materials science.[1] They are of particular relevance for application in frustrated Lewis pair chemistry.[2] Especially, Lewis acids that exceed the fluoride ion affinity (FIA) of SbF_5, so-called *Lewis superacids* (LSAs), are of current interest.[4] Promising LSAs based on boron,[5] aluminum,[4a,6] or cationic group 15 elements[7] have been demonstrated in recent years. Very strong Lewis acids based on neutral silicon species are much less developed. The Lewis acidity at silicon can be enhanced by three strategies: (1) strong electron withdrawing substituents,[8] (2) incorporation of silicon in strained cycles[9] or (3) transient activation *via* Lewis base coordination.[10] For example, the use of perfluoroaryl substituents in $(C_6F_5)_nSiF_{4-n}$ was reported by Frohn and Dilman.[11] Hoge demonstrated the C_2F_5 group as a robust substituent for the generation of strong silicon Lewis acids.[13] Although bis(catecholato)silanes have been known for several decades, their Lewis acidity was realized only in a recent seminal work by Tilley.[14] Therein, bis(perfluorocatecholato) silane **Si(cat^{F})$_2$** (Fig. 1) was demonstrated as a catalyst for the hydrosilylation of electron-poor aldehydes. Encouraged by the fact that aromatic chloro substituents have a weaker π-overlap with aromatic systems than fluorides, our group addressed bis(perchlorocatecholato)silane **Si(cat^{Cl})$_2$**.[3] According to its computed and experimental FIA in comparison to other neutral silanes, **Si(cat^{Cl})$_2$** represented the first silane exceeding the affinity of SbF_5, thus being the first neutral silicon Lewis superacid. Many well-defined pentacoordinate[12,15] and hexacoordinate[16] complexes based on silicon catecholates have been characterized much earlier. Pentacoordinate anionic bis(catecholato)silicates were used as hydride or allyl donors to carbonyls,[17] and more recently for the photoredox catalytic

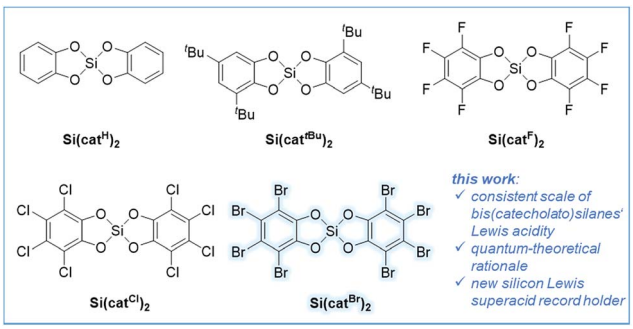

Fig. 1 Bis(catecholato)silanes Si(cat^{X})$_2$ are synthesized and assessed for their Lewis acidity in this work, and the herein introduced new Lewis superacid record holder is Si(cat^{Br})$_2$; derivatives with X = Cl, Br were isolated as CH_3CN-bis-adducts.

Anorganisch-Chemisches Institut, Ruprecht-Karls-Universität Heidelberg, Im Neuenheimer Feld 275, 69120 Heidelberg, Germany. E-mail: greb@uni-heidelberg.de

† Electronic supplementary information (ESI) available: Experimental, crystallographic and computational details. CCDC 1905749–1905760. For ESI and crystallographic data in CIF or other electronic format see DOI: 10.1039/c9sc02167a

generation of alkyl radicals.[18] The related tris(catecholato) silicate dianions have in fact been known for almost 100 years and serve as a prime example for hexacoordination of silicon.[19] Obviously, the Lewis acidity of the underlying catecholatosilanes is decisive for the stability and reactivity of all their adducts. However, a general account of the Lewis acidity of bis(catecholato)silanes is missing in the literature.

The present work provides a systematic experimental and theoretical study of the Lewis acidity of bis(catecholato)silanes. Even the weakest derivative **Si(cat^{H})$_2$** is uncovered as sufficiently Lewis acidic to form an anionic chlorosilicate. More important, the limit of Lewis acidity with neutral silicon species is pushed beyond that of the previous LSA record holder **Si(cat^{Cl})$_2$**. All experimental findings and the origin of the Lewis acidity of bis(catecholato)silanes are rationalized by state-of-the-art quantum theoretical tools.

Results and discussion

Synthesis of bis(catecholato)silanes

The syntheses of variably substituted bis(catecholato)silanes **Si(cat^{X})$_2$** (Fig. 1) were performed by a standard procedure (Scheme 1). Two equivalents of the respective catechols in acetonitrile were reacted with $HSiCl_3$ for 1 h at room temperature, followed by the release of gaseous by-products (H_2, HCl). The reaction was continued for 12 h at 40 °C, leading to the precipitation of the desired bis(catecholato)silanes as acetonitrile adducts from the reaction mixture. Washing of the precipitates with acetonitrile and CH_2Cl_2 was performed to remove residual HCl and unreacted catechol. In the case of X = H, 3,5-^{t}Bu and F, complete release of CH_3CN was possible upon exposure to high-vacuum conditions, whereas for X = Cl, Br two equivalents of CH_3CN remained in the samples. Based on this method, the derivatives **Si(cat^{X})$_2$**($\cdot 2CH_3CN$) (X = H, 3,5-^{t}Bu, F, Cl, Br) were accessible in good yields at multigram scale (76–89%). The pronounced affinity towards acetonitrile gave the first hints of the exceptional Lewis acidity of **Si(cat^{Cl})$_2$** and **Si(cat^{Br})$_2$**. The poor solubility of the derivatives **Si(cat^{X})$_2$**($\cdot 2CH_3CN$) in non-donor solvents prevented full NMR spectroscopic analysis of the free Lewis acids. However, NMR spectroscopy in donor solvents, mass spectrometry and elemental analysis confirmed the composition **Si(cat^{X})$_2$** or **Si(cat^{X})$_2$**$\cdot 2CH_3CN$ for the formed precipitates and were in agreement with previous literature reports.[3,14,15i,20] The new Lewis acid **Si(cat^{Br})$_2$** was additionally characterized by X-ray diffraction as a bis-adduct with diethyl ether (see ESI†). Depending on the reaction conditions, bis(catecholato)silanes have been proposed as either monomeric,[15i,16c,20a,21] oligomeric[20a,22] or polymeric.[23] However, facile depolymerization of the oligomers was believed to occur in the presence of Lewis bases.[20a,24]

Although the presence of oligomers or aggregates in the formed precipitates cannot be ruled out herein, it is believed that the presence of acetonitrile as the reaction medium stabilizes the monomeric **Si(cat^{X})$_2$** species *via* coordination, in particular for the halogenated derivatives (X = F, Cl, Br). Most convincingly, the addition of various neutral or anionic donors (*vide infra*) to the obtained powders led to the exclusive formation of donor→**Si(cat^{X})$_2$** species without the detection of any side products. The remainder of this work exploits the defined donor→**Si(cat^{X})$_2$** adducts to assess the inherent Lewis acidity of the **Si(cat^{X})$_2$** species by effective, global and intrinsic scaling methods.[4b]

Preparation of adducts and the scaling of the Lewis acidity of bis(catecholato)silanes

The Lewis acidity of a compound can be inspected by the spectroscopic response of a suitable probe molecule bound to the acceptor side – the so-called *effective scaling method*.[4b] As was discussed previously, the ν(CN) IR-stretching mode of CH_3CN-adducts does not provide a meaningful scaling – and was not considered herein.[4b] Although the Gutmann–Beckett (GB) method[25] also has its shortcomings due to its dependence on steric effects or "Pearson hardness", it enables a reasonable scaling of the Lewis acidity within one class of compounds.[4b] Hence, the triethylphosphine oxide adducts of **Si(cat^{X})$_2$** were prepared by the addition of varying amounts of Et_3PO (0.5 to 3.0 eq.) in CD_2Cl_2. Depending on the amount of added Et_3PO, two major species were identified: the mono-adduct Et_3PO–**Si(cat^{X})$_2$** and the bis-adduct Et_3PO–**Si(cat^{X})$_2$**–$OPEt_3$, further verified by X-ray structural analysis (*vide infra*). For the non-halogenated Lewis acids **Si(cat^{H})$_2$** and **Si(cat^{tBu})$_2$**, a single averaged ^{31}P-NMR signal was visible, which continuously shifted upon increasing the amount of Et_3PO, indicating a fast exchange

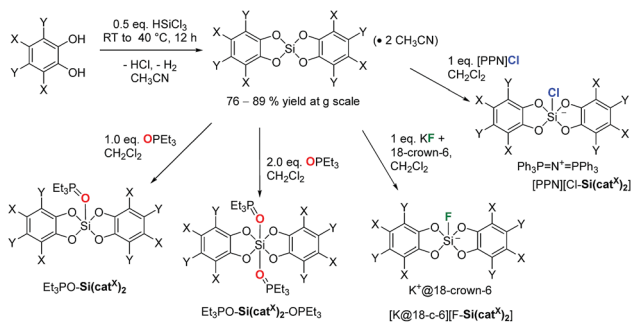

Scheme 1 The synthesis of the herein described species (X/Y = H, F, Cl, Br or H/^{t}Bu).

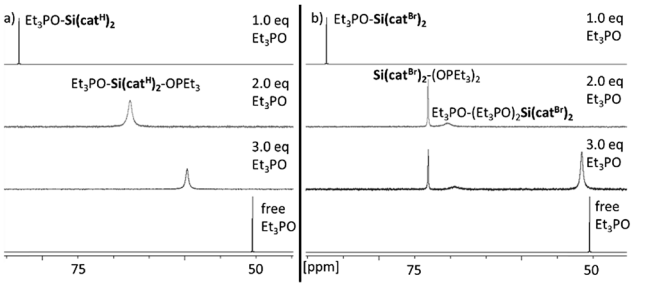

Fig. 2 Changes in the ^{31}P-NMR spectra for samples of (a) **Si(cat^{H})$_2$** and 1.0–3.0 eq. of Et_3PO, and (b) **Si(cat^{Br})$_2$** and 1.0–3.0 eq. of Et_3PO in CD_2Cl_2.

between the different adducts and free Et_3PO at the NMR time scale (see Fig. 2a for **Si(cat^{H})$_2$** and Fig. S1† for **Si(cat^{tBu})$_2$**). For the halogenated Lewis acids **Si(cat^{X})$_2$** (X = F, Cl, Br), distinct signals for the mono- ($\delta \approx 86$ ppm) and bis-adducts ($\delta \approx 73$ ppm) were observable, indicating stronger binding (see Fig. 2b for **Si(cat^{Br})$_2$** and Fig. S2/S3† for **Si(cat^{F})$_2$**/**Si(cat^{Cl})$_2$**). In addition, a minor species ($\delta \approx 70$ ppm) was visible for the halogenated Lewis acids, proposed as a coordination product of a third Et_3PO in the second coordination sphere of the *cis* bis-adduct Et_3PO–**Si(cat^{X})$_2$**–$OPEt_3$ (see ESI†).[26] The chemical shifts of the ^{31}P-NMR signals of the mono-adducts Et_3PO–**Si(cat^{X})$_2$** were chosen as the probe for the GB method (see Fig. S4†). According to the induced shift relative to the free Et_3PO, a ranking for **Si(cat^{X})$_2$** of X = 3,5-^{t}Bu < H ≪ F < Cl < Br was obtained (Table 1).

This is an interesting finding, as it supported the hypothesis of increasing Lewis acidity with decreasing π-backbonding capability of the substituents X in the catechols. Indeed, the σ_m Hammett parameters for the respective substituents X (Table 1, last column) are in line with the observed Lewis acidity trend.[27]

The mono-fluoride adducts of the bis(catecholato)silanes [K@18-crown-6][**F-Si(cat^{X})$_2$**] were obtained by the addition of 1 eq. KF and 18-crown-6 to **Si(cat^{X})$_2$**(·2CH_3CN) in CH_2Cl_2 at room temperature and subsequent precipitation with pentanes. The fluorosilicates were characterized by heteronuclear NMR spectroscopy, ESI-MS and (except for X = ^{t}Bu) X-ray diffraction. The ^{19}F-NMR chemical shifts are all around −133 ppm and the ^{29}Si-NMR chemical shifts of around −90 ppm lie in the expected range for pentacoordinate silicates (Table 2). Interestingly, the $^{1}J_{SiF}$ coupling constants (189–195 Hz) correlate with the Lewis acidity trend obtained by the GB method, and indicate an increased covalent interaction between silicon and fluoride (as is further supported in the computational section). The ^{19}F-NMR spectra of trigonal-bipyramidal [**F-Si(cat^{tBu})$_2$**]$^-$ with an unsymmetrically substituted catechol revealed two *trans* isomers (95%) which are in mutual exchange by Berry pseudo-rotation and 5% of the *cis* form (see Fig. S5†).[28]

The respective chlorosilicates [PPN][**Cl-Si(cat^{X})$_2$**] were accessible by reacting 1 eq. bis(triphenylphosphoranylidene)ammonium chloride ([PPN]Cl) with **Si(cat^{X})$_2$**(·2CH_3CN) in CH_2Cl_2 for 24 h at room temperature and subsequent precipitation with pentanes. The adduct formation was verified by heteronuclear NMR spectroscopy and in the case of [PPN][**Cl-Si(cat^{H})$_2$**] also by X-ray diffraction. The respective ^{29}Si-NMR chemical shifts lie in the range of pentacoordinate silanes (see Table 2) and are in agreement with the computed ^{29}Si-NMR shifts (see Table S4†). Intriguingly, those compounds belong to the rare class of anionic chlorosilicates. Due to the large solvation free energy of the chloride ion, it usually needs strong silicon Lewis acids to stabilize the respective chlorosilicates in solution, as was demonstrated for the first time only in 2014 with perfluoroethyl-substituted silanes.[29] Remarkably, the acceptor strengths of even the weakest bis(catecholato)silanes, **Si(cat^{H})$_2$** and **Si(cat^{tBu})$_2$**, are sufficient to achieve this goal.

Table 1 Measured ^{31}P-NMR chemical shifts for the monoadducts Et_3PO–Si(cat^{X})$_2$ in CD_2Cl_2 in reference to free Et_3PO; σ_m Hammett parameters for the catechol substituents X[a]

Si(cat^{X})$_2$–$OPEt_3$	δ ^{31}P-NMR [ppm]	Δ [ppm]	σ_m of X[27]
Si(cat^{tBu})$_2$	81.6	31.1	−0.100
Si(cat^{H})$_2$	83.2	32.7	0.000
Si(cat^{F})$_2$	86.6	36.1	0.337
Si(cat^{Cl})$_2$	87.2	36.7	0.373
Si(cat^{Br})$_2$	87.3	36.8	0.391

[a] Blind sample of Et_3PO in CD_2Cl_2 (162 MHz): δ ^{31}P-NMR = 50.5 ppm.

With the range of halide adducts, the relative solution phase fluoride ion affinities (FIA_{sol}) and chloride ion affinities (CIA_{sol}) were addressed by competition experiments. The five Lewis acids were grouped into two sets: X = H, 3,5-^{t}Bu, F (set 1) and X = F, Cl, Br (set 2). Within one set, all possible combinations of 1 eq. fluoride adduct [**F-Si(cat^{X})$_2$**]$^-$ and 1 eq. of another Lewis acid, **Si(cat^{Y})$_2$**(·2CH_3CN), were mixed in CD_2Cl_2, and the ratio of the respective fluoride adducts [**F-Si(cat^{X})$_2$**]$^-$ and [**F-Si(cat^{Y})$_2$**]$^-$ was obtained by ^{19}F-NMR peak integration (after a minimum of 36 h at rt, ESI Section 1.2.6†). The assignment of the peaks was accomplished by comparison with the known ^{19}F-NMR spectra of the pure compounds [**F-Si(cat^{X})$_2$**]$^-$. In addition, a prominent third singlet appeared between the expected two ^{19}F-NMR signals of the fluoride adducts [**F-Si(cat^{X})$_2$**]$^-$ and [**F-Si(cat^{Y})$_2$**]$^-$. The origin of this signal was identified as the product [**F-Si(cat^{X})(cat^{Y})**]$^-$ resulting from a catecholato exchange reaction. Indeed, identical products formed statistically after mixing of equimolar amounts of two fluoride adducts [**F-Si(cat^{X})$_2$**]$^-$/[**F-Si(cat^{Y})$_2$**]$^-$. Catecholato scrambling in anionic hypercoordinate silicon catecholates was proposed by Woollins *et al.*, but not further verified.[28] Herein, evidence of the process was provided by ^{19}F/^{29}Si-NMR spectroscopy, ESI-MS and in the case of [K@18-crown-6][**F-Si(cat^{F})(cat^{Br})**] by X-ray structural analysis. Despite this catecholato scrambling, the competition experiments allowed for a meaningful interpretation of the relative FIA_{sol}. In particular, consideration of the results of the back and forth reaction of a specific pair provided sound conclusions. For example, the 1 : 1 mixture of [**F-Si(cat^{F})$_2$**]$^-$ and **Si(cat^{Br})$_2$**·2CH_3CN led to a distribution of 17% of [**F-Si(cat^{F})$_2$**]$^-$, 30% of [**F-Si(cat^{Br})$_2$**]$^-$ and 53% of heteroleptic [**F-Si(cat^{Br})(cat^{F})**]$^-$. In the respective back reaction (a combination of [**F-Si(cat^{Br})$_2$**]$^-$ and **Si(cat^{F})$_2$**), almost no fluoride exchange occurred (only 4% of [**F-Si(cat^{F})$_2$**]$^-$ formed after 36 h), besides 41% of the catecholate scrambling product. Based on the product distributions in the mixtures for all considered combinations (back and forth), a FIA_{sol} trend of ^{t}Bu < H ≪ F < Cl < Br (Table 3) was obtained. Strikingly, this trend is in agreement with the results of the GB method. Analogous competition reactions were performed with the chloride adducts [PPN][**Cl-Si(cat^{X})$_2$**], yielding the same relative order for the CIA_{sol} (see Table S2†).

Description of solid-state structures

Multiple X-ray diffraction analyses of pentacoordinate and hexacoordinate neutral and anionic donor→**Si(cat^{X})$_2$** species were performed. In the following, the structural parameters of relevance will be discussed. Those are in particular the donor

Table 2 Experimental ^{19}F- and ^{29}Si-NMR parameters for the anionic fluoro- and chlorosilicates of **Si(cat^{X})$_2$** in CD_2Cl_2

[Z-**Si(cat^{X})$_2$**]$^-$	δ ^{19}F-NMR (Z = F)	δ ^{29}Si-NMR (Z = F)	$^1J_{SiF}$ [Hz] (Z = F)	δ ^{29}Si-NMR (Z = Cl)
Si(cat^{tBu})$_2$	−131.6; −133.7, −133.9	−104.8	188.9	−91.8
Si(cat^{H})$_2$	−133.1	−104.8	191.1	−91.6
Si(cat^{F})$_2$	−133.5	−101.6	194.8	−87.1
Si(cat^{Cl})$_2$	−132.7	−105.1	195.2	−90.4
Si(cat^{Br})$_2$	−132.3	−107.0	195.2	−92.5

atom-Si and the Si–O_{cat} bond lengths. In addition, the distortion of trigonal-bipyramidal (tbp) to square-pyramidal (sp) (in the present case, more precisely, rhomboid-pyramidal) along the so-called Berry coordinate will be compared for all pentacoordinate species.

By crystallization of mixtures of **Si(cat^{X})$_2$** with less than 1.0 eq. of Et_3PO in CH_2Cl_2/pentanes, the mono-adducts Et_3PO–**Si(cat^{X})$_2$** for X = H, F and Br were obtained (Fig. 3a for X = Br). The Si–O_{cat} bond lengths are similar for all the adducts and lie in the typical range of pentacoordinate silicon catecholates.[24] The donor–acceptor Si–O_5 bond lengths, as well as the phosphorus–oxygen bond lengths of the coordinated phosphine oxides (P–O5), do not correlate with the induced ^{31}P-NMR chemical shifts of the GB method (Table 4). For the Et_3PO–**Si(cat^{F})$_2$** adduct, two independent donor–acceptor pairs are present in the unit cell, for which the Si–O5 and the P–O5 bond lengths in fact differ by 0.02 Å. These observations emphasize the inability to discuss Lewis acidities in terms of solid-state structural parameters due to the small curvature of the potential energy surface at its minimum in donor–acceptor bonding.[30] By crystallization of **Si(cat^{X})$_2$** combined with 2.0 eq. of Et_3PO in CH_2Cl_2/pentanes, single crystals of the bis-adducts Et_3PO–**Si(cat^{X})$_2$**–$OPEt_3$ for X = H, F, Cl and Br were obtained (Fig. 3b, for X = Br). All complexes show an almost ideal octahedral coordination sphere with an inversion center at silicon (C_i point group). As expected for hexacoordinate silicon structures, the Si–O_{cat} bond lengths are longer than the respective ones in the corresponding pentacoordinate species. The Si–O3 bond lengths are also longer than the ones in the Et_3PO mono-adducts. Again, they do not correlate with the obtained Lewis acidity trend. The P–O3 bond lengths are shorter than in the Et_3PO–**Si(cat^{X})$_2$** mono-adducts in all cases. The anionic fluorosilicates [K@18-crown-6][**F-Si(cat^{X})$_2$**] were crystallized by vapor diffusion of pentanes into saturated solutions of dichloromethane (Fig. 3c for X = F). The coordination geometries around silicon lie between tbp and sp, with the fluoride anions consequently occupying the apical position in the sp structures, and the equatorial positions in the tbp arrangements. [K@18-crown-6][**F-Si(cat^{F})$_2$**] was crystallized in two polymorphs A and B: in polymorph A (Fig. 3c), the [K@18-crown-6]$^+$ unit is coordinated to the apical fluoride F1 at silicon, whereas in polymorph B (Fig. 3d), one cationic unit is coordinated to a fluoro substituent at catechol and another unit has the closest contact to the π-system of another catechol, overall forming a coordination polymer. The product of the catecholato scrambling, [K@18-crown-6][**F-Si(cat^{F})(cat^{Br})**], shows two different [K@18-crown-6]$^+$ units, one bridging two anions by K–F1 interaction, and one unit stacked between two $O_2C_6F_4$ rings (only one of the two independent cationic units is shown in Fig. 3e). The Si–F bond lengths compared for all fluorosilicates are again not in correlation with the experimental solution phase Lewis acidities (Table 4). The strongest impact on the Si–F bond length seems to be interaction with the potassium.

Table 3 Measured product distribution (in %) of fluorosilicates obtained by ^{19}F-NMR signal integration after >36 h in CD_2Cl_2 between the reactants given in column 1[a]

[**F-Si(cat^{X})$_2$**]$^-$ + **Si(cat^{Y})$_2$**	[**F-Si(cat^{X})$_2$**]$^-$	[**F-Si(cat^{Y})$_2$**]$^-$	[**F-Si(cat^{X}) (cat^{Y})**]$^-$	rel. FIA_{sol}
X = H, Y = ^{t}Bu	65	<1	35	H > ^{t}Bu
X = ^{t}Bu, Y = H	<1	70	30	
X = H, Y = F	20	76	4	F > H
X = F, Y = H	>99	<1	0	
X = ^{t}Bu, Y = F	<1	72	28	F > ^{t}Bu
X = F, Y = ^{t}Bu	>99	<1	<1	
X = F, Y = Cl	21	27	52	Cl > F
X = Cl, Y = F	49	8	43	
X = F, Y = Br	17	30	53	Br > F
X = Br, Y = F	55	5	40	
X = Cl, Y = Br	20	29	51	Br > Cl
X = Br, Y = Cl	58	4	38	

[a] 0.05 M of [K@18-c-6][F-**Si(cat^{X})$_2$**] and 0.05 M **Si(cat^{Y})$_2$** in CD_2Cl_2, room temp., min. 36 h equilibration time, for Y = Cl and Br, the CH_3CN adducts were used.

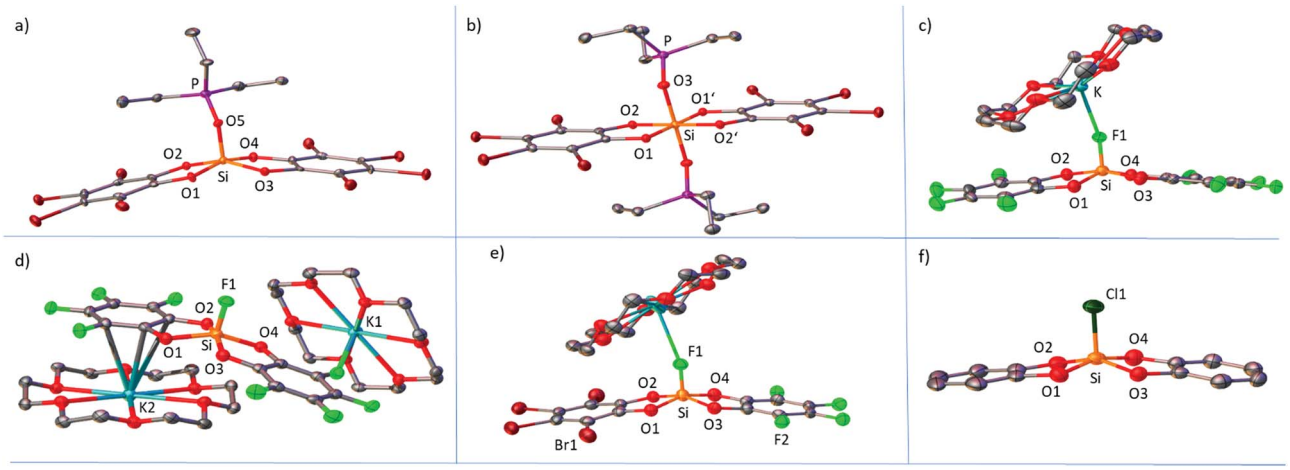

Fig. 3 Representative solid-state molecular structures of (a) Et_3PO–**Si(cat^{Br})$_2$**, (b) Et_3PO–**Si(cat^{Br})$_2$**–$OPEt_3$, and (c) [K@18-crown-6][**F-Si(cat^{F})$_2$**], polymorph A; (d) selection of the unit cell of [K@18-crown-6][**F-Si(cat^{F})$_2$**], polymorph B, (e) [K@18-crown-6][**F-Si(cat^{Br})(cat^{F})**], and (f) [PPN][**Cl-Si(cat^{H})$_2$**], cation omitted for clarity (ellipsoids at 50% probability level, hydrogen atoms omitted for clarity).

Structures in which the Si–F is coordinated to potassium ([**F-Si(cat^{F})$_2$**]$^-$ polymorph A, [**F-Si(cat^{Cl})$_2$**]$^-$ and [**F-Si(cat^{Br})$_2$**]$^-$) generally show longer Si–F bonds than structures wherein the [K@18-crown-6]$^+$ is coordinated elsewhere ([**F-Si(cat^{H})$_2$**]$^-$ and [**F-Si(cat^{F})$_2$**]$^-$ polymorph B). Single crystals of the anionic chlorosilicate [PPN][**Cl-Si(cat^{H})$_2$**] were obtained by overlayering a dichloromethane solution with pentanes (Fig. 3f). The coordination geometry around silicon is strongly distorted towards sp, with the chloride in the apical position. The Si–Cl bond length is rather on the short side (2.104 Å) in comparison to the

Table 4 Selected bond lengths (in Å), angles (in °) and topology parameters (TP) of the Et_3PO-mono and bis-adducts, fluorosilicates and the chlorosilicate of bis(catecholato)silanes as obtained by X-ray diffraction analyses

Et_3PO–**Si(cat^{X})$_2$**	X = H	X = F (unit 1)	X = F (unit 2)	X = Br	$(Et_3PO)_2$–**Si(cat^{X})$_2$**	X = H	X = F	X = Cl[3]	X = Br
Si–O5	1.709(2)	1.688(2)	1.694(2)	1.702(4)	Si–O3	1.863(2)	1.823(2)	1.832(1)	1.836(2)
P–O5	1.560(2)	1.544(2)	1.557(2)	1.550(3)	P–O3	1.526(2)	1.523(2)	1.533(1)	1.535(2)
Si–O1	1.745(2)	1.727(2)	1.746(2)	1.726(3)	Si–O1	1.754(1)	1.767(2)	1.766(1)	1.763(2)
Si–O2	1.705(2)	1.733(2)	1.726(2)	1.734(3)	Si–O2	1.757(1)	1.768(1)	1.763(1)	1.766(2)
Si–O3	1.737(2)	1.721(2)	1.727(2)	1.713(3)					
Si–O4	1.709(2)	1.731(2)	1.725(2)	1.723(3)					
O1–Si–O2	89.6(1)	89.5(1)	89.2(1)	89.3(2)	O1–Si–O2	90.7(1)	90.8(1)	90.6(1)	90.4(1)
O3–Si–O4	89.8(1)	89.7(1)	90.1(1)	90.3(2)	O1–Si–O2′	89.3(1)	89.3(1)	89.4(1)	89.6(1)
O1–Si–O4	87.0(1)	86.2(1)	85.4(1)	87.1(2)	O2–Si–O3	88.5(1)	88.3(1)	88.9(1)	89.0(1)
O2–Si–O3	87.0(1)	85.0(1)	85.6(1)	84.5(2)	O2′–Si–O3	91.4(1)	91.8(1)	91.1(1)	91.0(1)
O1–Si–O3	170.3(1)	154.2(1)	156.8(1)	158.5(2)					
O2–Si–O4	140.2(1)	158.3(1)	155.7(1)	156.3(2)					
TP (% tbp)	0.50	0.02	0.02	0.04					

[**F-Si(cat^{X})$_2$**]$^-$	X = H[12]	X = F (Poly A)	X = F (Poly B)	X = Cl[3]	X = Br	X = F/Br	[**Cl-Si(cat^{X})$_2$**]$^-$	X = H
Si–F1	1.600(8)	1.600(1)	1.609(2)	1.606(1)	1.610(2)	1.604(4)	Si–Cl1	2.104(2)
Si–O1	1.767(8)	1.731(1)	1.742(2)	1.731(1)	1.751(3)	1.736(4)	Si–O1	1.711(4)
Si–O2	1.746(9)	1.745(1)	1.720(2)	1.738(1)	1.724(3)	1.731(4)	Si–O2	1.735(4)
Si–O3	1.686(8)	1.728(1)	1.746(2)	1.739(1)	1.743(3)	1.739(5)	Si–O3	1.720(3)
Si–O4	1.720(8)	1.741(1)	1.718(2)	1.738(1)	1.734(3)	1.732(4)	Si–O4	1.736(4)
O1–Si–O2	88.9(1)	89.4(1)	89.6(1)	89.1(1)	89.0(1)	89.0(2)	O1–Si–O2	89.9(2)
O3–Si–O4	89.5(1)	89.3(1)	89.6(1)	89.0(1)	89.0(1)	89.1(2)	O3–Si–O4	89.0(2)
O1–Si–O4	86.4(1)	85.5(1)	85.4(1)	85.7(1)	84.4(1)	85.5(2)	O1–Si–O4	85.7(2)
O2–Si–O3	88.0(1)	86.3(1)	85.7(1)	85.6(1)	87.4(1)	85.8(2)	O2–Si–O3	85.2(2)
O1–Si–O3	133.1(5)	149.8(1)	162.3(1)	153.7(1)	160.9(1)	155.2(2)	O1–Si–O3	151.4(2)
O2–Si–O4	171.2(5)	161.8(1)	148.2(1)	156.5(1)	148.6(1)	155.1(2)	O2–Si–O4	159.1(2)
TP (% tbp)	0.64	0.20	0.24	0.05	0.21	0.00		0.12

few other structurally characterized chlorosilicates (2.100–2.218 Å).[29,31] The distortion of all pentacoordinate species from tbp to sp can be discussed by reference to a simple topology parameter (TP) along the so called Berry coordinate (a brief definition of the TP can be found in the ESI).[32] TP = 1 means an ideal tbp and TP = 0 an ideal sp structure. A clear distinction between the "weak" **Si(cat^{H})$_2$** and the stronger halogenated derivatives can be found. In agreement with earlier observations, the pentacoordinate halogenated derivatives are much more distorted towards the sp form (Table 4).[33] Therein, a stabilization of the sp form, which is usually higher in energy, is attributed to the diminished electron density at the mutually repulsing oxygen atoms in the basal plane.[12] This is in line with the stronger π-back donation of the free electron pairs to the aromatic ring systems in the halogenated derivatives. However, no clear trend is observed within the class of halogenated derivatives, due to the predominant effect of crystal packing forces and the low tbp–sp deformation energy.[34]

Comparison of bis(catecholato)silanes in chloride abstraction and catalytic hydrodefluorination

As an additional Lewis acidity scaling method, the reactions of **Si(cat^{X})$_2$** towards trityl chloride in CD_2Cl_2 were investigated. The weaker Lewis acids **Si(cat^{H})$_2$** and **Si(cat^{tBu})$_2$** did not induce significant ionization of trityl chloride, whereas with the halogenated derivatives, strongly colored solutions and clear NMR signals of the trityl cation developed. Although isolation of the formed salts was not possible, the amount of trityl cation in solution was easily determined by ^{1}H-NMR signal integration (Table 5 and Fig. S6†). Whereas the previous scaling methods and computations (see below) indicated a larger CIA for **Si(cat^{Cl})$_2$** *vs.* **Si(cat^{F})$_2$**, in the chloride abstraction experiments **Si(cat^{F})$_2$** and **Si(cat^{Cl})$_2$**·2CH_3CN displayed similar efficiency. This observation might be explained by the poor solubility of **Si(cat^{Cl})$_2$**·2CH_3CN in the absence of a suitable donor and/or the competing adduct formation with acetonitrile. Importantly, the highest ratio of chloride abstraction was clearly observed with the new Lewis acid **Si(cat^{Br})$_2$**·2CH_3CN.

To compare the catalytic efficiencies of the halogenated Lewis acids, the reaction profile of the hydrodefluorination reaction (3 mol% **Si(cat^{X})$_2$**) of 1-adamantylfluoride with 2 eq. of Et_3SiH in CD_3CN at 75 °C) was followed (Fig. 4). The efficiencies for **Si(cat^{F})$_2$** and **Si(cat^{Cl})$_2$** were similar, which again might be caused by the poorer solubility of **Si(cat^{Cl})$_2$**·2CH_3CN. The early

Table 5 Amount of trityl cation formed by chloride abstraction from trityl chloride with **Si(cat^{X})$_2$**(·2CH_3CN), obtained by ^{1}H-NMR signal integration in CD_2Cl_2, 21 mM

Si(cat^{X})$_2$(·2CH_3CN) + Ph_3CCl ⇌ [Ph_3C][**Cl-Si(cat^{X})$_2$**]

X =	% of Ph_3C^+
F	62
Cl	60
Br	83

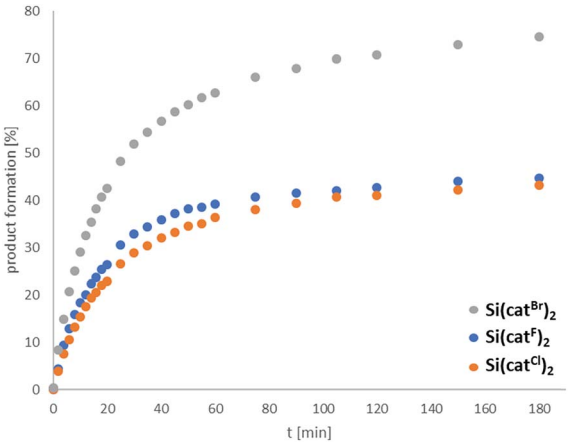

Fig. 4 Catalytic hydrodefluorination reaction of 1-adamantylfluoride with 2 eq. Et_3SiH and 3 mol% **Si(cat^{X})$_2$** in CD_3CN (0.26 M) at 75 °C. Reaction progress obtained by ^{19}F-NMR peak integration against C_6F_6 as an internal standard.

cessation of the reaction progress, the need for catalyst loadings of min. 10 mol% to complete the reaction and the observation of decomposition products *via* ^{19}F-NMR spectroscopy all indicated low turnover number (TON) for X = F, Cl. In contrast, the catalytic performance of **Si(cat^{Br})$_2$** was markedly superior, both in terms of estimated TON and turnover frequency (TOF). Although the full mechanistic and kinetic analysis of this reaction is beyond the scope of the present contribution, these results clearly reveal the efficiency and robustness of **Si(cat^{Br})$_2$** for future catalytic applications. It might be surprising that the **Si(cat^{X})$_2$** catalysts show poorer performance in this hydrodefluorination reaction compared to boranes like $B(C_6F_5)_3$ or 9-BBN – which are rated less Lewis acidic by FIA or GB.[35] However, two points are of note here: (1) Lewis acidity is ill-defined for parametrization along a single dimension. It is governed by three (partially) independent variables: charge density, orbital energies/localization and sterics.[4b] The parameters of Lewis acidity that result in high FIA or GB numbers do not necessarily impart high catalytic efficiency. This efficiency is often governed by orbital mixing terms, which profit from localized LUMO shapes and low lying LUMO energies (soft Lewis acidity). (2) The FIA and GB numbers reflect thermodynamic parameters, whereas catalytic efficiencies are also influenced by the reaction kinetics.

Computational results

To obtain a meaningful theoretical scaling of the Lewis acidities of the species **Si(cat^{X})$_2$** (X = H, F, Cl, Br), the gas and solution phase FIA and CIA were computed at the accurate DLPNO-CCSD(T)/aug-cc-pVQZ//PW6B95-D3(BJ)/def2-TZVPP level of theory *via* the isodesmic reaction enthalpies. Previous benchmark studies revealed the PW6B95-D3(BJ)/def2-TZVPP level of theory as ideal for geometry optimization for this class of substances.[3] First, the dissociation free energies for CH_3CN from **Si(cat^{Cl})$_2$**·2CH_3CN were computed. Loss of the first CH_3CN was found to be endergonic (ΔG = 12 kJ mol^{-1}), but the dissociation of the second CH_3CN was exergonic (ΔG = −31 kJ mol^{-1}).

Consequently, dissociation of both CH_3CN units should occur under diluted conditions, and a discussion of the FIA trends based on the free Lewis acids should therefore be reasonable. To our delight, the FIA and CIA of the free Lewis acids **Si(cat^X)$_2$** with and without solvent correction were in agreement with our experimental findings (X = H ≪ F < Cl < Br, Table 6, FIA, for CIA see Table S3†). The computations further disclosed the perbrominated Lewis acid ***Si(cat^{Br})$_2$*** *as by far the strongest of all bis(catecholato)silanes*, which represents the new record holder of reachable Lewis superacidity with neutral silanes. The same trend was obtained for the respective chloride ion affinities (see Table S3†). To provide a rationale for the origin of the high affinity of bis(catecholato)silanes, stepwise structural variations starting from SiH_4 were performed *in silico* and the effect on the FIA was investigated. The FIA of SiH_4 was arbitrarily set to zero. The nature of bonding between silicon and the fluoride ion in the respective fluorosilicates was concomitantly inspected by energy decomposition analyses (EDA, see Table 6).[36] The exchange of the hydrides in SiH_4 for methoxy groups in $Si(OMe)_4$ induced an increase of the FIA by 35 kJ mol^{-1}. This is caused by a stronger positive polarization of the silicon center, leading to a more pronounced Coulomb interaction with the negative fluoride ion (Table 6, orange shade). Because of the extra space provided to the free electron pairs at the oxygen atoms *via* delocalization in $Si(OPh)_4$, the FIA increases significantly. This is a consequence of diminished Pauli repulsion in the respective adduct, strengthening the overall interaction between the fluoride and the silane (Table 6, blue shade). The geometric effect in the spiro compounds **Si(cat^X)$_2$** again increases the FIA significantly. The ring closure reduces the formation energy in comparison to $Si(OPh)_4$ and increases the absolute amounts of Coulomb and orbital interaction in the fluoride adducts (Table 6, purple shade). The halogenation of the catechol backbone does not change the ratio of electrostatic to orbital contributions in the Si–F bonding, but increases both of their absolute values simultaneously.

To rationalize the dependence of the FIA on the substituents X in the catechol backbone, the electronic structures of the **[F-Si(cat^X)$_2$]$^-$** anions were analyzed further by natural bond orbital (NBO) methods.[37] In particular, the p_z-type natural localized molecular orbitals (NLMOs) at oxygen were inspected. The delocalization tails of the NLMOs at oxygen towards silicon decrease with X in the order H ≥ F > Cl > Br (expressed by the % of participation at silicon for this NLMO, Table 6, red shade). At the same time, the second order perturbation energy of the free p_z(O) NBO towards the aromatic π*-CC orbitals increases in the same order (Table 6, green shade). This finding is in agreement with the hypothesis of decreased π-electron density in the order X = H > F > Cl > Br, which is empirically manifested by the increasing Hammett constants of the substituents X. When substituting the aromatic rings with weaker π-donors, but still suitable σ-acceptors, the free electron pairs at oxygen favorably delocalize in the aromatic ring systems instead of competing with the fluoride ion at silicon to occupy accessible space, which would lead to a weaker Si–F bond and a weaker Lewis acid. The strong inductive effect of the electronegative oxygen atoms remains unaffected by the groups X and guarantees the overall strong positive polarization of the silicon center.

Analysis of all fluoridosilicates by the quantum theory of atoms in molecules (QTAIM) was performed next. It generally revealed closed shell ionic interactions for the silicon–fluoride bonds (Table 6).[38] The Laplacian of the electron density ∇^2 at the bond critical point of the Si–F bonds increases with increasing Lewis acidity – which is characteristic for enforced ionic bonding.[38b,39] However, in addition, the electron density ρ and the delocalization index δ between silicon and fluoride increase according to the same trend. Both observations reveal enforced covalent bonding upon enhancement of FIA/Lewis acidity. The simultaneous increase of ionic and covalent bonding effects – orthogonal not antipodal – has been described only recently in the context of the silicon–oxygen bond.[40] It is also operative in

Table 6 Computed FIA of silicon-based Lewis acids and Si(cat^X)$_2$, values of energy decomposition analysis (EDA), natural bond orbital (NBO) analysis and quantum theory of atoms in molecules (QTAIM) (for details, see ESI)

		EDA[c]				NBO[e]		QTAIM (Si-F bond)[h]		
Compound[a]	FIA[b]	Pauli[d]	Coulomb (%)[d]	Orbital (%)[d]	E_{prep}[d]	%NLMO[f]	E^2 LP(O) --> CC*[g]	$\rho(r_{BCP})$	$\nabla^2(r_{BCP})$	δ
SiH_4	177 (78)	184	-148 (60)	-100 (40)	19	--	--	0.097	0.56	0.286
$Si(OMe)_4$	212 (88)	183	-177 (64)	-100 (36)	44	--	--	0.100	0.59	0.210
$Si(OPh)_4$	302[i] (127)	148	-151 (58)	-107 (41)	53	--	--	0.121	0.77	0.252
$Si(cat^H)_2$	391 (241)	249	-223 (58)	-160 (42)	38	8.40	77.5	0.135	0.94	0.300
$Si(cat^F)_2$	490 (302)	229	-224 (58)	-163 (42)	40	8.40	80.4	0.139	0.97	0.307
$Si(cat^{Cl})_2$[j]	507 (315)	233	-224 (57)	-169 (43)	40	8.04	89.6	0.139	0.98	0.308
$Si(cat^{Br})_2$[j]	538 (347)	255	-242 (58)	-172 (41)	38	7.97	92.3	0.140	0.99	0.308

[a] Geometries at PW6B95-D3/def2-TZVPP. [b] DLPNO-CCSD(T)/aug-cc-pVQZ, values in brackets corrected for solvation (COSMO-RS/CH_2Cl_2). [c] BP86-D/TZ2P. [d] kcal mol^{-1}. [e] PBE0-D3/def2-TZVPP. [f] % of all p_z(O) NLMO at Si. [g] Second order perturbation energy of p_z(O) to π*(CC) in aromatic ring [kcal mol^{-1}]. [h] PBE0-D3/def2-TZVPP electron densities, values in atomic units. [i] cc-pVQZ basis set (see ESI). [j] Isolated as acetonitrile adducts.

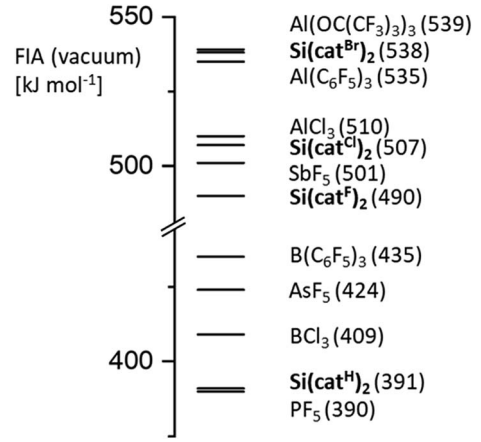

Fig. 5 Comparison of FIA of the $Si(cat^X)_2$ class with other selected Lewis acids (all values obtained at DLPNO-CCSD(T)/aug-cc-pVQZ level of theory).

this case, providing the silicon bis(catecholates) with their Lewis acidity.

To evaluate an *intrinsic* scale for the Lewis acidity of all studied silanes, the global electrophilicity index (GEI) was computed.[41] As can be seen in Fig. S11,† the GEI yields a good correlation with the FIA within the class of bis(catecholato) silanes and thus provides a shortcut tool for a rapid preliminary assessment. However, it fails for the comparison with the other classes of silanes which have been investigated computationally during this work.

Conclusions

We herein provide the first general account of the Lewis acidity of bis(catecholato)silanes – a class of substances that is easily accessible by a one-step protocol in high yields. A combined experimental and theoretical study of effective, global and intrinsic Lewis acidity measures gives a consistent *Lewis acidity trend for* $Si(cat^X)_2$ *of* $X = {}^tBu < H \ll F < Cl < Br$. Their FIAs range between moderate strengths like that of PF_5 (X = H) to extreme Lewis acidity like $Al(OC(CF_3)_3)_3$ (X = Br) (Fig. 5, further reference FIA data can be found in ref. 4*b*). Thus, we herein identified and synthesized the Lewis acid $Si(cat^{Br})_2$, which constitutes a new record holder of reachable Lewis acidity within neutral silanes. Inspection of the solid-state structures reemphasized the inability of structural parameters to accurately reflect Lewis acidity. Finally, this contribution demonstrates a correlation between the Lewis acidity of the investigated bis(catecholato)silanes and their efficiency in halide abstraction reactions and catalytic applications. Although the presence of acetonitrile in the strongest acids (X = Cl, Br) might limit their compatibility with very reactive cations, applicability in manifold transformations can be conceived.

The applied theoretical analyses provide a rationale for the origin of the FIA in bis(catecholato)silanes and deliver inspiration for future modifications within this class of Lewis acids. Contradicting the general notion that the inductive effects of the substituents X (F > Cl > Br) are decisive, it is rather the decreasing ability of X for π-backdonation into the catechol aromatic system (F > Cl > Br) that dominates the observed Lewis acidities. These insights might guide future design principles for even stronger Lewis acids.

Conflicts of interest

There are no conflicts to declare.

Acknowledgements

We gratefully thank Prof. H.-J. Himmel for his support, the FCI and DFG for financial support and the BWFor/BWUniCluster for computational resources. D. H. thanks the FES for a PhD scholarship.

References

1 (*a*) H. Yamamoto, *Lewis acids in organic synthesis*, Wiley-VCH, Weinheim, 2002; (*b*) A. Corma and H. García, *Chem. Rev.*, 2003, **103**, 4307–4366; (*c*) J. Eames and M. Watkinson, in *Metalloenzymes and electrophilic catalysis*, John Wiley & Sons Ltd, 2007, vol. 1, pp. 508–519; (*d*) H. Yamamoto and K. Ishihara, *Acid catalysis in modern organic synthesis*, Wiley-VCH, Weinheim, 2008; (*e*) E. Y.-X. Chen, in *Frustrated Lewis Pairs II: Expanding the Scope*, ed. G. Erker and D. W. Stephan, Springer Berlin Heidelberg, Berlin, Heidelberg, 2013, pp. 239–260.

2 (*a*) D. W. Stephan, *J. Am. Chem. Soc.*, 2015, **137**, 10018–10032; (*b*) D. W. Stephan and G. Erker, *Angew. Chem., Int. Ed.*, 2015, **54**, 6400–6441.

3 R. Maskey, M. Schädler, C. Legler and L. Greb, *Angew. Chem., Int. Ed.*, 2018, **57**, 1717–1720.

4 (*a*) L. O. Müller, D. Himmel, J. Stauffer, G. Steinfeld, J. Slattery, G. Santiso-Quiñones, V. Brecht and I. Krossing, *Angew. Chem., Int. Ed.*, 2008, **47**, 7659–7663; (*b*) L. Greb, *Chem.–Eur. J.*, 2018, **24**, 17881–17896.

5 L. A. Körte, J. Schwabedissen, M. Soffner, S. Blomeyer, C. G. Reuter, Y. V. Vishnevskiy, B. Neumann, H.-G. Stammler and N. W. Mitzel, *Angew. Chem., Int. Ed.*, 2017, **56**, 8578–8582.

6 (*a*) T. Belgardt, J. Storre, H. W. Roesky, M. Noltemeyer and H.-G. Schmidt, *Inorg. Chem.*, 1995, **34**, 3821–3822; (*b*) G. S. Hair, A. H. Cowley, R. A. Jones, B. G. McBurnett and A. Voigt, *J. Am. Chem. Soc.*, 1999, **121**, 4922–4923; (*c*) A. Wiesner, T. W. Gries, S. Steinhauer, H. Beckers and S. Riedel, *Angew. Chem., Int. Ed.*, 2017, **56**, 8263–8266; (*d*) J. F. Kogel, D. A. Sorokin, A. Khvorost, M. Scott, K. Harms, D. Himmel, I. Krossing and J. Sundermeyer, *Chem. Sci.*, 2018, **9**, 245–253.

7 (*a*) C. B. Caputo, L. J. Hounjet, R. Dobrovetsky and D. W. Stephan, *Science*, 2013, **341**, 1374–1377; (*b*) B. Pan and F. P. Gabbaï, *J. Am. Chem. Soc.*, 2014, **136**, 9564–9567.

8 (*a*) A. D. Dilman and S. L. Ioffe, *Chem. Rev.*, 2003, **103**, 733–772; (*b*) L. Ratjen, M. van Gemmeren, F. Pesciaioli and

B. List, *Angew. Chem., Int. Ed.*, 2014, **53**, 8765–8769; (*c*) D. Höfler, M. v. Gemmeren, P. Wedemann, K. Kaupmees, I. Leito, M. Leutzsch, J. B. Lingnau and B. List, *Angew. Chem., Int. Ed.*, 2017, **56**, 1411–1415.

9 (*a*) A. G. Myers, S. E. Kephart and H. Chen, *J. Am. Chem. Soc.*, 1992, **114**, 7922–7923; (*b*) K. Matsumoto, K. Oshima and K. Utimoto, *J. Org. Chem.*, 1994, **59**, 7152–7155; (*c*) J. W. A. Kinnaird, P. Y. Ng, K. Kubota, X. Wang and J. L. Leighton, *J. Am. Chem. Soc.*, 2002, **124**, 7920–7921; (*d*) X. Zhang, K. N. Houk and J. L. Leighton, *Angew. Chem., Int. Ed.*, 2005, **44**, 938–941; (*e*) R. Hrdina, C. E. Müller, R. C. Wende, K. M. Lippert, M. Benassi, B. Spengler and P. R. Schreiner, *J. Am. Chem. Soc.*, 2011, **133**, 7624–7627; (*f*) W. A. Chalifoux, S. K. Reznik and J. L. Leighton, *Nature*, 2012, **487**, 86.

10 (*a*) S. E. Denmark and T. Wynn, *J. Am. Chem. Soc.*, 2001, **123**, 6199–6200; (*b*) S. E. Denmark and G. L. Beutner, *J. Am. Chem. Soc.*, 2003, **125**, 7800–7801; (*c*) S. E. Denmark, G. L. Beutner, T. Wynn and M. D. Eastgate, *J. Am. Chem. Soc.*, 2005, **127**, 3774–3789; (*d*) A. V. Malkov, A. J. Liddon, P. Ramirez-Lopez, L. Bendova, D. Haigh and P. Kocovsky, *Angew. Chem., Int. Ed.*, 2006, **45**, 1432–1435; (*e*) S. E. Denmark and G. L. Beutner, *Angew. Chem., Int. Ed.*, 2008, **47**, 1560–1638; (*f*) R. Hrdina, F. Opekar, J. Roithova and M. Kotora, *Chem. Commun.*, 2009, 2314–2316.

11 (*a*) H. J. Frohn, M. Giesen, A. Klose, A. Lewin and V. V. Bardin, *J. Organomet. Chem.*, 1996, **506**, 155–164; (*b*) A. D. Dilman, V. V. Levin, M. Karni and Y. Apeloig, *J. Org. Chem.*, 2006, **71**, 7214–7223; (*c*) A. D. Dilman, V. V. Levin, A. A. Korlyukov, P. A. Belyakov, M. I. Struchkova, M. Y. Antipin and V. A. Tartakovsky, *J. Organomet. Chem.*, 2008, **693**, 1005–1019.

12 U. Dettlaff-Weglikowska, E. Hey-Hawkins and H. G. von Schnering, *Z. Naturforsch., B: J. Chem. Sci.*, 1991, **46**, 609.

13 (*a*) M. Wiesemann and B. Hoge, *Chem.–Eur. J.*, 2018, **24**, 16457–16471; (*b*) S. Steinhauer, J. Bader, H.-G. Stammler, N. Ignat'ev and B. Hoge, *Angew. Chem., Int. Ed.*, 2014, **53**, 5206–5209; (*c*) N. Schwarze, B. Kurscheid, S. Steinhauer, B. Neumann, H. G. Stammler, N. Ignat'ev and B. Hoge, *Chemistry*, 2016, **22**, 17460–17467; (*d*) B. Waerder, M. Pieper, L. A. Körte, T. A. Kinder, A. Mix, B. Neumann, H.-G. Stammler and N. W. Mitzel, *Angew. Chem., Int. Ed.*, 2015, **54**, 13416–13419.

14 A. L. Liberman-Martin, R. G. Bergman and T. D. Tilley, *J. Am. Chem. Soc.*, 2015, **137**, 5328–5331.

15 (*a*) C. L. Frye, *J. Am. Chem. Soc.*, 1964, **86**, 3170–3171; (*b*) C. M. S. Yoder and J. J. Zuckerman, *Inorg. Chem.*, 1967, **6**, 163–164; (*c*) F. P. Boer, J. J. Flynn and J. W. Turley, *J. Am. Chem. Soc.*, 1968, **90**, 6973–6977; (*d*) J. J. Harland, R. O. Day, J. F. Vollano, A. C. Sau and R. R. Holmes, *J. Am. Chem. Soc.*, 1981, **103**, 5269–5270; (*e*) R. R. Holmes, R. O. Day, J. J. Harland and J. M. Holmes, *Organometallics*, 1984, **3**, 347–353; (*f*) R. R. Holmes, R. O. Day, J. J. Harland, A. C. Sau and J. M. Holmes, *Organometallics*, 1984, **3**, 341–347; (*g*) R. R. Holmes, R. O. Day, V. Chandrasekhar, J. J. Harland and J. M. Holmes, *Inorg. Chem.*, 1985, **24**, 2016–2020; (*h*) K. C. K. Swamy, V. Chandrasekhar, J. J. Harland, J. M. Holmes, R. O. Day and R. R. Holmes, *J. Am. Chem. Soc.*, 1990, **112**, 2341–2348; (*i*) E. Hey-Hawkins, U. Dettlaff-Weglikowska, D. Thiery and H. G. von Schnering, *Polyhedron*, 1992, **11**, 1789–1794; (*j*) R. Tacke, J. Becht, A. Lopez-Mras and J. Sperlich, *J. Organomet. Chem.*, 1993, **446**, 1–8; (*k*) J. H. Small, D. J. McCord, J. Greaves and K. J. Shea, *J. Am. Chem. Soc.*, 1995, **117**, 11588–11589; (*l*) R. Tacke, M. Pülm and B. Wagner, in *Adv. Organomet. Chem.*, ed. R. West and A. F. Hill, Academic Press, 1999, vol. 44, pp. 221–273; (*m*) J. B. Lambert and S. R. Singer, *J. Organomet. Chem.*, 2004, **689**, 2293–2302.

16 (*a*) F. Carré, G. Cerveau, C. Chuit, R. J. P. Corriu and C. Réyé, *Angew. Chem., Int. Ed.*, 1989, **28**, 489–491; (*b*) S. P. Narula, R. Shankar, M. Kumar and Meenu, *Inorg. Chem.*, 1994, **33**, 2716–2718; (*c*) F. E. Hahn, M. Keck and K. N. Raymond, *Inorg. Chem.*, 1995, **34**, 1402–1407.

17 (*a*) M. Kira, K. Sato and H. Sakurai, *J. Org. Chem.*, 1987, **52**, 948–949; (*b*) M. Kira, K. Sato and H. Sakurai, *J. Am. Chem. Soc.*, 1990, **112**, 257–260.

18 (*a*) V. Corcé, L.-M. Chamoreau, E. Derat, J.-P. Goddard, C. Ollivier and L. Fensterbank, *Angew. Chem.*, 2015, **127**, 11576–11580; (*b*) M. Jouffroy, D. N. Primer and G. A. Molander, *J. Am. Chem. Soc.*, 2016, **138**, 475–478; (*c*) C. Leveque, L. Chenneberg, V. Corce, C. Ollivier and L. Fensterbank, *Chem. Commun.*, 2016, **52**, 9877–9880.

19 (*a*) A. Rosenheim and O. Sorge, *Ber. Dtsch. Chem. Ges.*, 1920, **53**, 932–939; (*b*) A. Rosenheim, B. Raibmann and G. Schendel, *Z. Anorg. Allg. Chem.*, 1931, **196**, 160–176; (*c*) A. Weiss, G. Reiff and A. Weiss, *Z. Anorg. Allg. Chem.*, 1961, **311**, 151–179; (*d*) H. Bartels and H. Erlenmeyer, *Helv. Chim. Acta*, 1964, **47**, 7–13; (*e*) J. J. Flynn and F. P. Boer, *J. Am. Chem. Soc.*, 1969, **91**, 5756–5761; (*f*) D. W. Barnum, *Inorg. Chem.*, 1972, **11**, 1424–1429; (*g*) D. F. Evans, J. Parr and E. N. Coker, *Polyhedron*, 1990, **9**, 813–823; (*h*) J. V. Kingston, B. Vargheese and M. N. S. Rao, *Main Group Chem.*, 2000, **3**, 79–90; (*i*) R. Tacke and O. Seiler, in *Silicon Chemistry*, ed. U. Schubert and P. Jutzi, Wiley-VCH, 2007.

20 (*a*) H. R. Allcock, T. A. Nugent and L. A. Smeltz, *Synthesis and Reactivity in Inorganic and Metal-Organic Chemistry*, 1972, vol. 2, pp. 97–104; (*b*) A. K. Chekalov, A. I. Prokof'ev, N. N. Bubnov, S. P. Solodovnikov, A. A. Zhdanov and M. I. Kabachnik, *Bull. Acad. Sci. USSR, Div. Chem. Sci.*, 1981, **30**, 2064–2071.

21 H. Meyer and G. Nagorsen, *Angew. Chem., Int. Ed.*, 1979, **18**, 551–553.

22 (*a*) S. Robert and K. Wilhelm, *Z. Anorg. Allg. Chem.*, 1951, **266**, 185–192; (*b*) J. Mihailo, *Z. Anorg. Allg. Chem.*, 1957, **288**, 324–332; (*c*) J. J. Zuckerman, *J. Chem. Soc.*, 1962, 873–876.

23 W. Hönle, U. Dettlaff-Weglikowska, L. Walz and H. G. von Schnering, *Angew. Chem., Int. Ed.*, 1989, **28**, 623–624.

24 C. Y. Wong and J. D. Woollins, *Coord. Chem. Rev.*, 1994, **130**, 175–241.

25 (*a*) U. Mayer, V. Gutmann and W. Gerger, *Monatsh. Chem.*, 1975, **106**, 1235–1257; (*b*) M. A. Beckett, G. C. Strickland, J. R. Holland and K. Sukumar Varma, *Polymer*, 1996, **37**, 4629–4631.

26 E. L. Myers, C. P. Butts and V. K. Aggarwal, *Chem. Commun.*, 2006, 4434–4436.
27 H. C. Brown and Y. Okamoto, *J. Am. Chem. Soc.*, 1958, **80**, 4979–4987.
28 D. F. Evans, A. M. Z. Slawin, D. J. Williams, C. Y. Wong and J. D. Woollins, *J. Chem. Soc., Dalton Trans.*, 1992, 2383–2387.
29 S. Steinhauer, T. Böttcher, N. Schwarze, B. Neumann, H.-G. Stammler and B. Hoge, *Angew. Chem., Int. Ed.*, 2014, **53**, 13269–13272.
30 (*a*) V. Jonas, G. Frenking and M. T. Reetz, *J. Am. Chem. Soc.*, 1994, **116**, 8741–8753; (*b*) K. R. Leopold, M. Canagaratna and J. A. Phillips, *Acc. Chem. Res.*, 1997, **30**, 57–64; (*c*) D. G. Anderson, A. J. Blake, S. Cradock, E. A. V. Ebsworth, D. W. H. Rankin and A. J. Welch, *Angew. Chem., Int. Ed.*, 1986, **25**, 107–108.
31 T. Bottcher, S. Steinhauer, B. Neumann, H. G. Stammler, G. V. Roschenthaler and B. Hoge, *Chem. Commun.*, 2014, **50**, 6204–6206.
32 E. P. A. Couzijn, J. C. Slootweg, A. W. Ehlers and K. Lammertsma, *J. Am. Chem. Soc.*, 2010, **132**, 18127–18140.
33 R. Tacke, J. Heermann, M. Pülm and E. Gottfried, *Monatsh. Chem.*, 1999, **130**, 99–107.
34 R. Tacke, M. Pülm, I. Richter, B. Wagner and R. Willeke, *Z. Anorg. Allg. Chem.*, 1999, **625**, 2169–2177.
35 (*a*) C. B. Caputo and D. W. Stephan, *Organometallics*, 2012, **31**, 27–30; (*b*) S. S. Chitnis, F. Krischer and D. W. Stephan, *Chem.–Eur. J.*, 2018, **24**, 6543–6546.
36 (*a*) K. Kitaura and K. Morokuma, *Int. J. Quantum Chem.*, 1976, **10**, 325–340; (*b*) L. Zhao, M. Hermann, W. H. E. Schwarz and G. Frenking, *Nat. Rev. Chem.*, 2019, **3**, 48–63.
37 (*a*) A. E. Reed, L. A. Curtiss and F. Weinhold, *Chem. Rev.*, 1988, **88**, 899–926; (*b*) E. D. Glendening, C. R. Landis and F. Weinhold, *Wiley Interdiscip. Rev.: Comput. Mol. Sci.*, 2012, **2**, 1–42.
38 (*a*) R. F. W. Bader and H. Essén, *J. Chem. Phys.*, 1984, **80**, 1943–1960; (*b*) D. Stalke, *Chem.–Eur. J.*, 2011, **17**, 9264–9278.
39 C. Outeiral, M. A. Vincent, A. Martin Pendas and P. L. A. Popelier, *Chem. Sci.*, 2018, **9**, 5517–5529.
40 M. Fugel, M. F. Hesse, R. Pal, J. Beckmann, D. Jayatilaka, M. J. Turner, A. Karton, P. Bultinck, G. S. Chandler and S. Grabowsky, *Chemistry*, 2018, **24**, 15275–15286.
41 (*a*) R. G. Parr, L. v. Szentpály and S. Liu, *J. Am. Chem. Soc.*, 1999, **121**, 1922–1924; (*b*) P. K. Chattaraj, U. Sarkar and D. R. Roy, *Chem. Rev.*, 2006, **106**, 2065–2091; (*c*) A. R. Jupp, T. C. Johnstone and D. W. Stephan, *Dalton Trans.*, 2018, **47**, 7029–7035; (*d*) A. R. Jupp, T. C. Johnstone and D. W. Stephan, *Inorg. Chem.*, 2018, **57**, 14764–14771.